Cycloalkane-modified amphiphilic polymers provide direct extraction of membrane proteins for CryoEM analysis

Anna Higgins
University of Leeds
Alex Flynn
University of Leeds
Anaïs Marconnet
Université de Paris
Laura Musgrove
University of Leeds
Vincent Postis
University of Leeds
Jonathan Lippiat
University of Leeds https://orcid.org/0000-0003-3748-7345
Chun-Wa Chung
GlaxoSmithKline
Tom Ceska
UCB Pharma
Manuela Zoonens
Université de Paris
Frank Sobott
University of Leeds https://orcid.org/0000-0001-9029-1865
Stephen Muench (S.P.Muench@leeds.ac.uk)
University of Leeds https://orcid.org/0000-0001-6869-4414

Article

Keywords: CryoEM, membrane protein, amphipol, detergent

Posted Date: January 15th, 2021

DOI: https://doi.org/10.21203/rs.3.rs-131488/v1

Version of Record: A version of this preprint was published at Communications Biology on November 25th, 2021. See the published version at https://doi.org/10.1038/s42003-021-02834-3.

Abstract

Membrane proteins are essential for cellular growth and homeostasis, making up a large proportion of therapeutic targets. However, the necessity for a solubilising agent to extract them from the membrane creates significant challenges in their structural and functional study. Although amphipols have been very effective for single-particle electron cryo-microscopy (cryoEM) and mass spectrometry, they rely on initial detergent extraction before exchange into the amphipol environment. Therefore, circumventing this pre-requirement would be a significant advantage. Here we use a novel type of amphipol: a cycloalkane-modified amphiphile polymer (CyclAPol) to extract *Escherichia coli* AcrB directly from the membrane and demonstrate that the protein can be isolated in a one-step purification with the resultant cryoEM structure achieving 3.2 Å resolution. Together this work shows that cycloalkane amphipols provide a powerful detergent-free approach for the study of membrane proteins allowing native extraction and high-resolution structure determination by cryoEM.

Introduction

Membrane proteins represent ~ 30% of open reading frames in the human genome, ~ 70% of drug targets[1] and yet are only 3% of reported structures in the PDB. Despite their prevalence in the cell and importance for ion transport and cell signalling, amongst other functions they remain challenging research targets due to problems of overexpression, extraction and stabilisation of their native structure[2–5]. Traditionally extraction and purification of a membrane protein involves the use of a detergent, from which the protein may then be transferred into other surfactants, be they detergents of different chemical composition, protein-based nanodiscs or amphipols[6,7]. Extraction of a membrane protein into a detergent micelle functions by disrupting the interaction between protein and its surrounding lipid molecules[8]. Detergent molecules recover the hydrophobic surface of a membrane protein but poorly mimic the lipid bilayer in terms of lateral pressure and thickness[9] which has been shown to cause perturbations in the structure[9,10]. Moreover, the closely associated lipids which can be important for gating, regulation and stability, may be displaced by competition with the detergent[11–14]. In addition, detergent purification buffers must retain the detergent above its critical micelle concentration (CMC) in all downstream steps which may exacerbate lack of activity, dissociation of a protein complex, unnatural oligomerisation and loss of lipid cofactors, amongst other problems[15–17]. Detergent micelles in single-particle cryoEM lead to reduced contrast and increased noise[18,19] and must be disassembled in native mass spectrometry (MS)[20]. Due to the importance of membrane proteins and the problems associated with detergents, there exist several alternative membrane mimetics developed to circumvent this, of which the predominant are protein-based nanodiscs[21] and amphipathic polymers[22].

Classical amphipols (APols) are short and flexible amphipathic polymers able to form complexes with membrane proteins and maintain the proteins in a water-soluble form[22]. They have been established for decades[22,23] and are well-characterised in their applicability for stabilising membrane proteins. The prototypical APol A8-35 is a poly(acrylic acid) (PAA) polymer randomly modified with octylamine and

isopropylamine side chains[23], and many different functionalities have been tethered to the polymer for specific purposes[24,25]. In cryo-EM, APol A8-35 facilitated the first high-resolution single-particle structure of a membrane protein, that of TRPV1[26]. Since then, the number of high-resolution cryoEM structures of membrane proteins using APols (mainly A8-35 and PMAL-C8)[27] has increased[28]. Of those cryoEM structures deposited within the EMDB, the best resolution achieved using classical APols is 2.17 Å[29]. In addition, APols are amenable to native electrospray ionization (ESI)-MS[30]. However, A8-35 and the other classical APols traditionally require initial detergent extraction of the protein[31]. Other polymers are under development, such as the novel acrylic acid and styrene polymers (AASTY)[32], but their applicability to cryoEM has been limited to ~ 18 Å resolution.

Conversely, the copolymerisation of styrene and maleic acid (SMA)[33] heralded the advent of “native” nanodiscs containing a protein directly extracted from the membrane, with its endogenous lipids and without the requirement for conventional detergents[34–39]. The styrene maleic acid lipid particles (SMALPs) formed[40] lend themselves to a plethora of biophysical techniques, including cryoEM[41,42]. However, SMALPs also have their limitations; they are more sensitive to pH extremes and divalent cations than PAA-derivative APols, making them incompatible for some activity assays[37,43] while no MA-derived polymers have yet been successfully applied to native MS. Although it has recently been demonstrated that A8-35 can be utilised following protein extraction with SMA[44], an APol-like polymer combining the extraction capability of SMA with the applications of A8-35 would be highly advantageous.

Here we demonstrate that the properties of A8-35 and SMA can be combined through novel cycloalkane-modified APols with SMALP-like properties for direct extraction[45]. Using *Escherichia coli* AcrB, we demonstrate that these novel APol derivatives (henceforth distinguished as CyclAPols) are capable of solubilising the protein of interest directly from the membrane. The CyclAPols can be utilised at exceptionally low concentrations (0.1–0.5%) decreasing purification costs, and minimizing the risk of destabilisation due to high APol concentrations[46,47]. We present the first cryoEM structure of a protein in CyclAPols, at 3.2 Å resolution, demonstrating their applicability to high-resolution structure determination, making these APols an important new tool in the study of membrane proteins.

Results

Novel amphipathic polymers can solubilise proteins directly from membranes

To ascertain if the novel CyclAPols (C_6-C_2-50 and C_8-C_0-50) in addition to A8-35, are capable of direct membrane solubilisation, *E. coli* membranes overexpressing the exporter AcrB were homogenised and incubated with each polymer before ultracentrifugation to remove insoluble material. Western blot analysis showed that all polymers are capable of solubilising membranes and extracting AcrB, with the amphipathic polymers CyclAPol C_6-C_2-50 and C_8-C_0-50 showing greater solubilisation efficacy than A8-35 (Figure. S1). Under the experimental conditions used, C_8-C_0-50 appeared to perform better than C_6-C_2-50.

Nevertheless, yield of CyclAPol-extracted AcrB is at an equivalent level to the previously characterised SMA polymer, despite significantly lower polymer concentration for CyclAPols.

The solubilisation conditions were repeated and a one-step purification with affinity resin was carried out of AcrB stabilised with each polymer. This one-step purification procedure with SMA has previously been observed to result in clean homogenous protein[44,48], with increased purity of SMA-solubilised AcrB relative to detergent[44]. While minor modifications were made to optimise buffers for compatibility with the polymers, purification with CyclAPols resulted in clear elution fractions containing relatively pure AcrB protein consistent with a one-step purification (Fig. 1). The resultant elution fractions of each purification were pooled and dialysed to remove imidazole and concentrated to ~ 1 mg/mL.

Negative stain electron microscopy was used to assess the homogeneity and stability of AcrB extracted and purified in CyclAPols C_6-C_2-50 and C_8-C_0-50 showing homogenous, monodisperse protein consistent with that observed for SMA, with less background contamination than typically observed for detergent micelles (Fig. 2). The low level of aggregation and low background observed in the negative stain data for the C_6-C_2-50, C_8-C_0-50 and SMA samples were indicative of a sample suitable for cryoEM. However, images of A8-35-purified AcrB showed large aggregates which likely contain several copies of AcrB and only a small percentage of monodispersed AcrB (Fig. 2b). The large aggregates suggest that A8-35 is not as efficient as CyclAPols or SMA at breaking apart the membrane. 2D classification of AcrB purified with C_6-C_2-50 (**e**) and C_8-C_0-50 (**f**) showed typical features to those seen with AcrB-SMA[49] along with increased high angle views, particularly for C_8-C_0-50 (**f**, green boxes).

Single particle cryoEM of AcrB in CyclAPol C_8-C_0-50

We next investigated if CyclAPols, like the classic APols such as A8-35 and PMAL-C8, were also capable of providing a suitable environment for high-resolution structure determination by cryoEM. Purified AcrB was vitrified on Quantifoil grids for single-particle cryo-EM analysis. While AcrB extracted and purified in A8-35 was not suitable for cryoEM due to particle aggregation, in screening of grids both CyclAPols exhibited sufficient particle distribution. AcrB in C_8-C_0-50 showed the best distribution and was taken forward for data collection. Consistently, the C_8-C_0-50 polymer marginally outperformed C_6-C_2-50, with slightly increased purity, yield (Fig. 1) and particle homogeneity as seen in negative stain (Fig. 2) and screening in cryoEM (Figure S2).

Following data collection, particle picking was carried out with CrYOLO, and extraction and further processing carried out in RELION. Approximately 400 k particles were initially extracted from 1837 micrographs. Following two rounds of 2D classification, ~ 200 k particles were selected for further 3D classification and processing. Initial 2D classes showed a clear AcrB trimer, with a good angular distribution within the data (Fig. 3a). It was noted that a small population of the 2D classes exhibited clear doublets of AcrB trimers (0.5-1%) which had previously been seen in negative stain studies of AcrB in SMA[49], but not reported in the published structures[41,42].

The resultant 3D reconstruction, processed with C1 symmetry, achieved a final global resolution of 3.2 Å with clearly resolved density for the secondary structure and in most cases the side-chains (Fig. 3c). The local resolution is lower at exterior helices, where density for the side-chains could not be unambiguously resolved. The previously derived EM structure of AcrB in SMA[41] was used as a starting point for model building and refinement, with the resultant model being highly similar to previously published AcrB structures[41,42,50]. The structure is asymmetric and exhibits a clear cavity at the interior of the trimer, which after model fitting was devoid of any significant density that could be assigned to lipids (Fig. 4). This is especially apparent when viewed from the base of the structure, where the trimeric pseudo-symmetry and resolved helices are very clear. Particularly, the structure appears well resolved at the transmembrane region.

Comparison to AcrB in other amphipathic environments

Comparing the refined structure, especially the chain C of the AcrB trimer, in C_8-C_0-50 to the previously published structures in SMA (6baj)[41] and saposin (6sgu)[50] using Chimera showed an RMSD of 0.7 and 1.5 Å respectively, reflecting their close similarity. Comparison of the maps (Figure S3) or overlay of the SMA and CyclAPol structures (Fig. 3d) demonstrates no significant difference between structures and only minor variation in loop regions. It is noted that in the reported cryo-EM structures of AcrB in SMA or saposin at comparable resolutions, lipids have been identified throughout the transmembrane region. However, there is no density observed for the polymer or for the lipid in the C_8-C_0-50 reconstruction (Fig. 4).

Discussion

Membrane proteins present significant challenges, not least in finding a suitable amphipathic environment that can directly extract the protein from the membrane and stabilise it in aqueous solution. Although classical APols such as A8-35 are effective in cryoEM, their typical reliance on detergents in the early stages of membrane extraction may be problematic. Using AcrB, we demonstrate that while classical APols such as A8-35, as long suspected[22], may directly extract proteins from the membrane but the yield of AcrB extracted with A8-35 is low, confirming the poor detergency property of A8-35. Solubilisation with A8-35 is also incomplete as large objects similar to small vesicles are observed by negative stain EM (Fig. 2), the size of which perhaps could be fine-tuned by A8-35 concentration (currently 0.5%). Although not suitable for single-particle cryoEM, the ability to fragment the membrane into larger rafts may be useful for other techniques such as AFM or mass spectrometry[51] but was beyond the scope of this study. In contrast to A8-35, the two CyclAPols tested are very effective at solubilising AcrB from the membrane at low concentrations (at estimated total protein/polymer ratio of 1:1 w/w). This is consistent with the previous finding that the novel CyclAPols are more efficient than A8-35 at extracting proteins from membrane, regardless of the target protein[45].

Importantly, the CyclAPols are still compatible with high-resolution cryoEM studies with the resultant 3.2 Å resolution structure of AcrB obtained in CyclAPol C_8-C_0-50 being in line with the highest reported

resolutions obtained with classical APols. Further this clearly indicates no detriment is observed for cryo-EM as this represents the joint highest resolution AcrB cryoEM structure[41,50]. We noted a significant improvement in resolution compared to our in-house AcrB-SMA cryoEM reconstructions, the highest resolution of which is ~ 4.0 A[42] and for which the data acquisition setup and data processing pipelines were comparable.

Interestingly, the CyclAPol C_6-C_2-50 was not only less amenable to purification than C_8-C_0-50, but while two data collections were attempted with this polymer, the best resolution obtained was 4.4 Å (Figure S2). As previously noted, while less doublets are visible in 2D classification, a higher proportion of the protein appears aggregated or in multimeric chains in purifications with this polymer contributing to a highly diffuse transmembrane region (Figure S2). This highlights how subtle differences in the chemistry between the two CyclAPols can have a significant effect on the downstream applications, but this effect may be protein dependant. The overall architecture of AcrB is near indistinguishable between reconstructions in C_6-C_2-50 and C_8-C_0-50, although at the lower resolution we may not observe subtle differences.

AcrB is an ideal model protein for such studies as it has been so widely characterised with high-resolution cryoEM structures being determined in SMA (3.2 Å),[41] saposin (3.2 Å)[50] and most recently in liposomes (3.9 Å)[52]. Studies in saposin[50] and liposomes[52] involve reconstitution subsequent to detergent purification. However, AcrB within liposomes also does not appear to show closely associated internal lipids, unlike structures determined in both saposin and SMA. There were also no identifiable lipids in CyclAPol-purified AcrB. The CyclAPols may outcompete the binding of lipids or, alternatively, lipids are present but undetectable due to flexibility and averaging in the EM reconstruction. Furthermore, in significant contrast to studies in liposomes, in which a great deal of optimisation of cryoEM conditions was required,[52] the cryoEM structure obtained in C_8-C_0-50 was the result of one batch of cryoEM grids with no subsequent optimisation.

The CyclAPols represent a new significant tool in the field of membrane proteins. They may come to represent an important alternative to detergent and SMA. They extract directly from the membrane, at low concentrations, and provide a clean purification of the membrane protein. Compared to the novel polymer AASTY[32], the significantly improved compatibility of CyclAPols with cryoEM shows that the hydrophilic/hydrophobic group alternance as well as the size dispersity of the polymer are not the key parameters for the sample quality. From biophysical assays it is suspected that the stability of the protein is improved in CyclAPols over SMA and the sample can now be analysed by native MS (unpublished data). Although cryoEM analysis exhibits trimeric AcrB stripped of surrounding lipids, how general this effect is will require further investigations using both different model proteins and techniques of direct detection of lipids such as thin layer chromatography. Further whilst lipids have been detected in other cryoEM studies of AcrB, it is possible these are not critical for the function, as AcrZ[50] or AcrA[53] may mediate interactions between AcrB and lipids. CyclAPols represent potential advantages over SMA-purification of proteins in applications, but also an improved native extraction to classical APols. We

present here the first foray into these novel Apol derivatives, anticipating wider applicability to membrane proteins still to be discovered.

Conclusions

Membrane proteins offer great challenges in their study, with a major limitation being in using a surfactant that can both solubilise and stabilise the protein of interest and also be applicable to a range of downstream analysis techniques. APols have a strong track record in their applicability to single particle cryoEM and mass spectrometry, but have relied on initial detergent extraction, which brings with it some limitations. Here we have shown that a modified cycloalkane APol negates the need for initial detergent extraction whilst maintaining the applicability to high resolution EM structures. This new generation of APols may provide an important new addition to the membrane protein toolkit and create new opportunities in membrane protein studies.

Methods

Polymer synthesis

Polymers C_6-C_2-50 and C_8-C_0-50 were synthesised as described in Marconnet *et al* [45]. In addition, we used the commercial amphipol A8-35 and DDM from Anatrace, and SMA (2:1) supplied unhydrolyzed from Cray Valley.

Preparation of E. coli membranes

E. coli membranes were prepared according to Chap. 3.4 of [54] following which membranes were resuspended in a minimal volume of buffer (50 mM Tris-HCl pH 8.0, 500 mM NaCl, 10% glycerol) and frozen for storage at -80°C. The total protein concentration of the resuspended membranes was measured using a bicinchoninic acid (BCA) assay as per the manufacturer's recommendations (Thermo Scientific).

AcrB purification

Purification of AcrB in SMA was carried out as described previously[44,48] but with 1% SMA. For purification in SMA, the solubilisation buffer was 50 mM Tris pH 8.0, 500 mM NaCl, 10% glycerol. Wash and elution buffers additionally contain 20 mM imidazole and 300 mM imidazole, respectively. Purification in amphipols was similar but buffers were modified to reduce the ionic strength. For this, the solubilisation buffer contained 20 mM Tris pH 8.0, 250 mM NaCl, 5% glycerol. Wash and elution buffers were supplemented with 10 mM imidazole and 300 mM imidazole, respectively. A second purification was also carried out, which provided the sample of AcrB in CyclAPol C_6-C_2-50 for cryoEM data collections. For this second purification, the protocol was largely similar but an extra resin wash was carried out with buffer containing 50 mM imidazole, and the elution was performed with 500 mM imidazole.

Purification was carried out with membranes homogenised in solubilisation buffer to 1 mg/mL. SMA or APol was added and samples were incubated for 2 hours at room temperature before ultracentrifugation at 100,000 × g for 1 hour at 4°C to remove insoluble material.

The soluble material was incubated with equilibrated cobalt resin overnight at 4°C. The flow-through was collected, the resin washed with 5 column volumes solubilisation buffer and 5 column volumes wash buffer before elution fractions were collected and analysed by SDS-PAGE. Elution fractions containing pure AcrB were pooled, dialysed overnight against solubilisation buffer at 4°C then concentrated using 100 kDa MWCO nitrocellulose concentrator (Merck) and the final concentration measured using a DS-11 Spectrophotometer (DeNovix).

Negative-stain electron microscopy

Purified AcrB was diluted to 50 µg/mL in solubilisation buffer. 3 µL of sample was applied to a glow-discharged carbon grid, incubated for 30 seconds and excess removed with blotting paper. The grid was washed with double-distilled water and stained with 1% uranyl acetate. Grids of APol-purified AcrB were imaged at 50 k magnification using a Tecnai G2-spirit T12 transmission electron microscope (FEI) fitted with a 120 keV Lab6 electron source and Ultra Scan 4000 CCD camera (Gatan). Grids of SMA-purified AcrB were imaged using a Tecnai F20 transmission electron microscope (FEI) fitted with a 200 keV FEG electron source and a CETA CMOS CCD camera (FEI).

Electron cryo-microscopy

1.2/1.3 cryo-electron microscopy (cryo-EM) grids (QUANTIFOILS) were prepared by glow discharging with a 208-carbon High Vacuum Carbon Coater (Cressington). Purified AcrB at ~ 1 mg/mL after solubilisation with 0.5% A8-35, 0.1% C_6-C_2-50 and 0.1% C_8-C_0-50 was applied to grids. Cryo-EM specimens were prepared with a FEI Vitrobot grid preparation robot at 4 °C and 100% humidity by applying 3 µl of sample (~ 1 mg/ml) to glow-discharged grids, blotting for 6 s with a blot force of 6 before freezing in liquid ethane. Grids were stored in liquid nitrogen and imaged subsequently using a Titan Krios G3i cryo transmission electron microscope (FEI) at 300 keV voltage equipped with a Gatan K2 Summit camera at the Astbury Biostructure Laboratory. Grids were screened to assess ice thickness, AcrB concentration, monodispersion and homogeneity.

Electron microscopy data acquisition

Movies were acquired in electron counting mode with a pixel size of 1.07 Å, an exposure rate of 6.6 electrons per pixel per second, and a total exposure time of 10 s divided in 40 frames. Frame alignment and exposure weighting were performed with Motioncor[55]. Contrast transfer function parameters were estimated from the exposure-weighted averages of movie frames with CTFFIND[56].

Image processing

Automated picking of particles was carried out using crYOLO with the general model trained on a subset of particles and picking threshold at 0.2. From 1837 micrographs 409113 particles were picked of which 402672 were extracted into Relion. Two rounds of 2D classification and three rounds of 3D classification

were carried out, reducing particle numbers to 100 k, prior to further refinement. The map for AcrB structure in SMA[41], EMD-7074, in a 256 pixel box and low-pass filtered to 30 Å was used as an initial model. The dataset was also processed in cryoSPARC[57], from the raw image stage, obtaining a similar resolution of 3.3 Å at the final stage of refinement. As cryoSPARC's own algorithms were used for automated picking and model generation this served as an internal control that no bias was imposed. The model was produced by manual fitting of 6baj, with lipids removed, into the map. One round of real space refinement in Phenix was performed before fitting in Coot. Side chains were deleted where unambiguous density was not observed. The construct used possesses 2 additional N-terminal residues and a C-terminus extension including a His-tag. However, these were not seen in the final map, and numbering was matched to the canonical *E. coli* sequence. The coordinates and map are deposited with access codes PDB 7B5P and EMDB 12043 respectively.

Declarations

Author Contributions: Conceptualisation and experimental design: S.P.M., F.S., A.J.H., A.F., J.L., and V.P; Polymer synthesis: A.M.; Performed experiments: A.F. and A.J.H..; Analysis of data and model refinement: A.J.H., A.F., S.P.M. Discussed the data and wrote the manuscript: all authors. All authors have read and agreed to the published version of the manuscript.

Acknowledgments:

We would like to acknowledge the Muench and Sobott labs for fruitful discussions, particularly Anton Calabrese and David Klebl. The authors thank the Astbury Biostructure Laboratory for their assistance with EM data collection. The FEI Titan Krios microscopes were funded by the University of Leeds (UoL ABSL award) and Wellcome Trust (108466/Z/15/Z). This work and AJH was funded through a BBSRC grant (BB/R018561/1/). The amphipol development in IBPC Paris was supported by the Centre National de la Recherche Scientifique (CNRS), Université de Paris (Université Paris 7), and the "Initiative d'Excellence" program from the French State (Grant "DYNAMO", ANR-11-LABX-0011-01).

Conflicts of Interest: The authors declare no conflict of interest.

References

1. Overington, J. P., Al-Lazikani, B. & Hopkins, A. L. How many drug targets are there? *Nat. Rev. Drug Discov.* (2006) doi:10.1038/nrd2199.
2. Tate, C. G. Practical considerations of membrane protein instability during purification and crystallisation. *Methods Mol. Biol.* (2010) doi:10.1007/978-1-60761-344-2_12.
3. Bill, R. M. *et al.* Overcoming barriers to membrane protein structure determination. *Nat. Biotechnol.* **29**, 335–340 (2011).
4. Rawson, S., Davies, S., Lippiat, J. D. & Muench, S. P. The changing landscape of membrane protein structural biology through developments in electron microscopy. *Molecular Membrane Biology*

(2016) doi:10.1080/09687688.2016.1221533.

5. Zoonens, M. & Miroux, B. Expression of membrane proteins at the Escherichia coli membrane for structural studies. *Methods Mol. Biol.* (2010) doi:10.1007/978-1-60761-344-2_4.
6. Bayburt, T. H. & Sligar, S. G. Membrane protein assembly into Nanodiscs. *FEBS Lett.* **584**, 1721–1727 (2010).
7. Popot, J.-L. Amphipols, Nanodiscs, and Fluorinated Surfactants: Three Nonconventional Approaches to Studying Membrane Proteins in Aqueous Solutions. *Annu. Rev. Biochem.* (2010) doi:10.1146/annurev.biochem.052208.114057.
8. Arnold, T. & Linke, D. The use of detergents to purify membrane proteins. *Current Protocols in Protein Science* (2008) doi:10.1002/0471140864.ps0408s53.
9. Chipot, C. *et al.* Perturbations of Native Membrane Protein Structure in Alkyl Phosphocholine Detergents: A Critical Assessment of NMR and Biophysical Studies. *Chemical Reviews* (2018) doi:10.1021/acs.chemrev.7b00570.
10. Cross, T. A., Sharma, M., Yi, M. & Zhou, H. X. Influence of solubilizing environments on membrane protein structures. *Trends in Biochemical Sciences* (2011) doi:10.1016/j.tibs.2010.07.005.
11. Hedger, G. & Sansom, M. S. P. Lipid interaction sites on channels, transporters and receptors: Recent insights from molecular dynamics simulations. *Biochim. Biophys. Acta - Biomembr.* (2016) doi:10.1016/j.bbamem.2016.02.037.
12. Willegems, K. & Efremov, R. G. Influence of Lipid Mimetics on Gating of Ryanodine Receptor. *Structure* (2018) doi:10.1016/j.str.2018.06.010.
13. Pliotas, C. *et al.* The role of lipids in mechanosensation. *Nat. Struct. Mol. Biol.* (2015) doi:10.1038/nsmb.3120.
14. Gupta, K. *et al.* The role of interfacial lipids in stabilizing membrane protein oligomers. *Nature* (2017) doi:10.1038/nature20820.
15. Baylon, J. L. *et al.* Atomic-level description of protein-lipid interactions using an accelerated membrane model. *Biochim. Biophys. Acta - Biomembr.* **1858**, 1573–1583 (2016).
16. Kurauskas, V. *et al.* How Detergent Impacts Membrane Proteins: Atomic-Level Views of Mitochondrial Carriers in Dodecylphosphocholine. *J. Phys. Chem. Lett.* (2018) doi:10.1021/acs.jpclett.8b00269.
17. Dorwart, M. R., Wray, R., Brautigam, C. A., Jiang, Y. & Blount, P. S. aureus MscL is a pentamer in vivo but of variable stoichiometries in vitro: Implications for detergent- solubilized membrane proteins. *PLoS Biol.* (2010) doi:10.1371/journal.pbio.1000555.
18. Gewering, T., Januliene, D., Ries, A. B. & Moeller, A. Know your detergents: A case study on detergent background in negative stain electron microscopy. *J. Struct. Biol.* **203**, 242–246 (2018).
19. Vinothkumar, K. R. & Henderson, R. Single particle electron cryomicroscopy: trends, issues and future perspective. *Q. Rev. Biophys.* **49**, (2016).
20. Konijnenberg, A. *et al.* Global structural changes of an ion channel during its gating are followed by ion mobility mass spectrometry. *Proc. Natl. Acad. Sci. U. S. A.* **111**, 17170–17175 (2014).

21. Denisov, I. G. & Sligar, S. G. Nanodiscs for structural and functional studies of membrane proteins. *Nat. Struct. Mol. Biol.* **23**, 481–486 (2016).
22. Popot, J.-L. *Membrane Proteins in Aqueous Solutions from detergents to amphipols. Biological and Medical Physics Biomedical Engineering* (2018). doi:10.1007/978-3-319-73148-3.
23. Tribet, C., Audebert, R. & Popot, J. L. Amphipols: Polymers that keep membrane proteins soluble in aqueous solutions. *Proc. Natl. Acad. Sci. U. S. A.* (1996) doi:10.1073/pnas.93.26.15047.
24. Zoonens, M. & Popot, J. L. Amphipols for Each Season. *J. Membr. Biol.* (2014) doi:10.1007/s00232-014-9666-8.
25. Della Pia, E. A., Hansen, R. W., Zoonens, M. & Martinez, K. L. Functionalized Amphipols: A Versatile Toolbox Suitable for Applications of Membrane Proteins in Synthetic Biology. *J. Membr. Biol.* (2014) doi:10.1007/s00232-014-9663-y.
26. Liao, M., Cao, E., Julius, D. & Cheng, Y. Structure of the TRPV1 ion channel determined by electron cryo-microscopy. *Nature* (2013) doi:10.1038/nature12822.
27. Nagy, J. K. *et al.* Use of amphipathic polymers to deliver a membrane protein to lipid bilayers. *FEBS Lett.* (2001) doi:10.1016/S0014-5793(01)02627-8.
28. Le Bon, C., Michon, B., Popot, J.-L. & Zoonens, M. Amphipathic Environments for Determining the Structure of Membrane Proteins by Single-Particle Electron Cryo-Microscopy. *submitted* **2**, (2020).
29. Owji, A. P. *et al.* Structural and functional characterization of the bestrophin-2 anion channel. *Nat. Struct. Mol. Biol.* (2020) doi:10.1038/s41594-020-0402-z.
30. Watkinson, T. G. *et al.* Systematic analysis of the use of amphipathic polymers for studies of outer membrane proteins using mass spectrometry. *Int. J. Mass Spectrom.* (2015) doi:10.1016/j.ijms.2015.06.017.
31. Le Bon, C., Marconnet, A., Masscheleyn, S., Popot, J. L. & Zoonens, M. Folding and stabilizing membrane proteins in amphipol A8-35. *Methods* (2018) doi:10.1016/j.ymeth.2018.04.012.
32. Smith, A. A. A. *et al.* Lipid Nanodiscs via Ordered Copolymers. *Chem* (2020) doi:10.1016/j.chempr.2020.08.004.
33. Knowles, T. J. *et al.* Membrane proteins solubilized intact in lipid containing nanoparticles bounded by styrene maleic acid copolymer. *J. Am. Chem. Soc.* (2009) doi:10.1021/ja810046q.
34. Jamshad, M. *et al.* Structural analysis of a nanoparticle containing a lipid bilayer used for detergent-free extraction of membrane proteins. *Nano Res.* **8**, 774–789 (2015).
35. Gulati, S. *et al.* Detergent free purification of ABC transporters. *Biochem J* **44**, 1–24 (2014).
36. Lee, S. C. *et al.* A method for detergent-free isolation of membrane proteins in their local lipid environment. *Nat. Protoc.* (2016) doi:10.1038/nprot.2016.070.
37. Dörr, J. M. *et al.* The styrene–maleic acid copolymer: a versatile tool in membrane research. *European Biophysics Journal* (2016) doi:10.1007/s00249-015-1093-y.
38. Jamshad, M. *et al.* Surfactant-free purification of membrane proteins with intact native membrane environment. *Biochem. Soc. Trans.* **39**, 813–818 (2011).

39. Rajesh, S., Knowles, T. & Overduin, M. Production of membrane proteins without cells or detergents. *N. Biotechnol.* **28**, 250–254 (2011).
40. Orwick-Rydmark, M. *et al.* Detergent-free incorporation of a seven-transmembrane receptor protein into nanosized bilayer lipodisq particles for functional and biophysical studies. *Nano Lett.* (2012) doi:10.1021/nl3020395.
41. Qiu, W. *et al.* Structure and activity of lipid bilayer within a membrane-protein transporter. *Proc. Natl. Acad. Sci. U. S. A.* **115**, 12985–12990 (2018).
42. Johnson, R. M. *et al.* Cryo-EM structure and molecular dynamics analysis of the fluoroquinolone resistant mutant of the acrb transporter from salmonella. *Microorganisms* (2020) doi:10.3390/microorganisms8060943.
43. Fiori, M. C., Jiang, Y., Altenberg, G. A. & Liang, H. Polymer-encased nanodiscs with improved buffer compatibility. *Sci. Rep.* (2017) doi:10.1038/s41598-017-07110-1.
44. Hesketh, S. J. *et al.* Styrene maleic-acid lipid particles (SMALPs) into detergent or amphipols: An exchange protocol for membrane protein characterisation. *Biochim. Biophys. Acta - Biomembr.* **1862**, 183192 (2020).
45. Marconnet, A. *et al.* Solubilization and stabilization of membrane proteins by cycloalkane-modified amphiphilic. (2020) doi:10.1021/acs.biomac.0c00929.
46. Popot, J. L. *et al.* Amphipols from a to Z*. *Annu. Rev. Biophys.* (2011) doi:10.1146/annurev-biophys-042910-155219.
47. Sverzhinsky, A. *et al.* Amphipol-Trapped ExbB–ExbD Membrane Protein Complex from Escherichia coli: A Biochemical and Structural Case Study. *J. Membr. Biol.* (2014) doi:10.1007/s00232-014-9678-4.
48. Parmar, M. *et al.* Using a SMALP platform to determine a sub-nm single particle cryo-EM membrane protein structure. *Biochim. Biophys. Acta - Biomembr.* **1860**, 378–383 (2018).
49. Postis, V. *et al.* The use of SMALPs as a novel membrane protein scaffold for structure study by negative stain electron microscopy. *Biochim. Biophys. Acta - Biomembr.* **1848**, 496–501 (2015).
50. Du, D. & Luisi, B. Interactions of a bacterial RND transporter with a transmembrane small protein in a lipid environment. *Struct. Des.* 1–10 (2020) doi:10.1016/j.str.2020.03.013.
51. Chorev, D. S. & Robinson, C. V. “Protein assemblies ejected directly from native membranes yield complexes for mass spectrometry”. *Science (80-.).* **362**, 829–834 (2018).
52. Yao, X., Fan, X. & Yan, N. Cryo-EM analysis of a membrane protein embedded in the liposome. *Proc. Natl. Acad. Sci. U. S. A.* (2020) doi:10.1073/pnas.2009385117.
53. Shi, X. *et al.* In situ structure and assembly of the multidrug efflux pump AcrAB-TolC. *Nat. Commun.* (2019) doi:10.1038/s41467-019-10512-6.
54. Postis, V. L. G., Rawlings, A. E., Lesiuk, A. & Baldwin, S. A. *Ion Channels: Methods and Protocols*. *Methods in Molecular Biology* vol. 998 (Humana Press, 2013).

55. Zheng, S. Q. *et al.* MotionCor2: Anisotropic correction of beam-induced motion for improved cryo-electron microscopy. *Nature Methods* (2017) doi:10.1038/nmeth.4193.
56. Rohou, A. & Grigorieff, N. CTFFIND4: Fast and accurate defocus estimation from electron micrographs. *J. Struct. Biol.* (2015) doi:10.1016/j.jsb.2015.08.008.
57. Punjani, A., Rubinstein, J. L., Fleet, D. J. & Brubaker, M. A. CryoSPARC: Algorithms for rapid unsupervised cryo-EM structure determination. *Nat. Methods* **14**, 290–296 (2017).

Figures

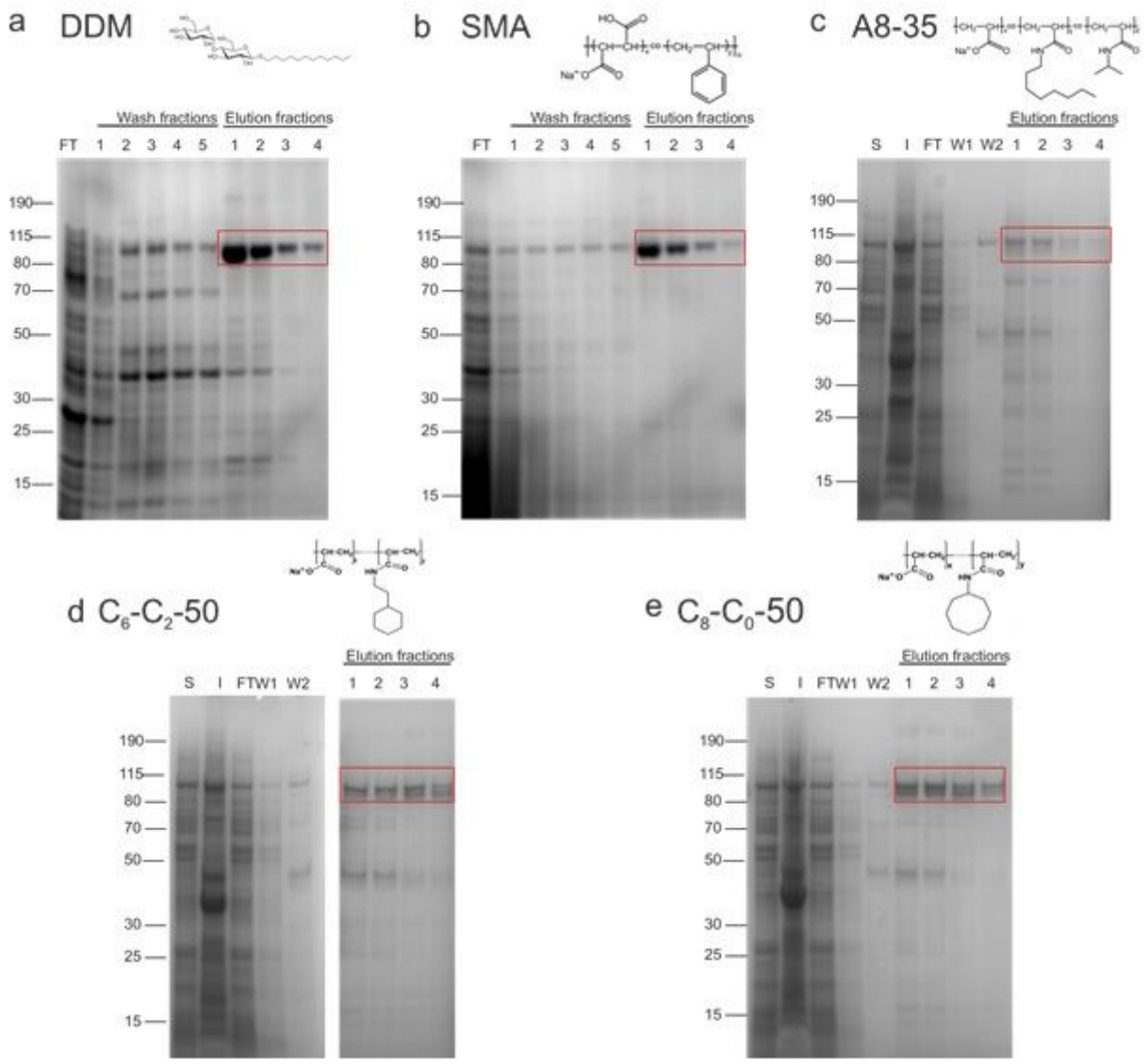

Figure 1

Purification of AcrB in different stabilizing systems. SDS-PAGE of purification of AcrB in a) DDM b) SMA c) A8-35 d) C6-C2-50 and e) C8-C0-50. Purification is shown with flow-through (FT) from affinity beads,

and wash (W) steps, in addition to soluble (S) and insoluble (I) samples for the amphipol purifications.

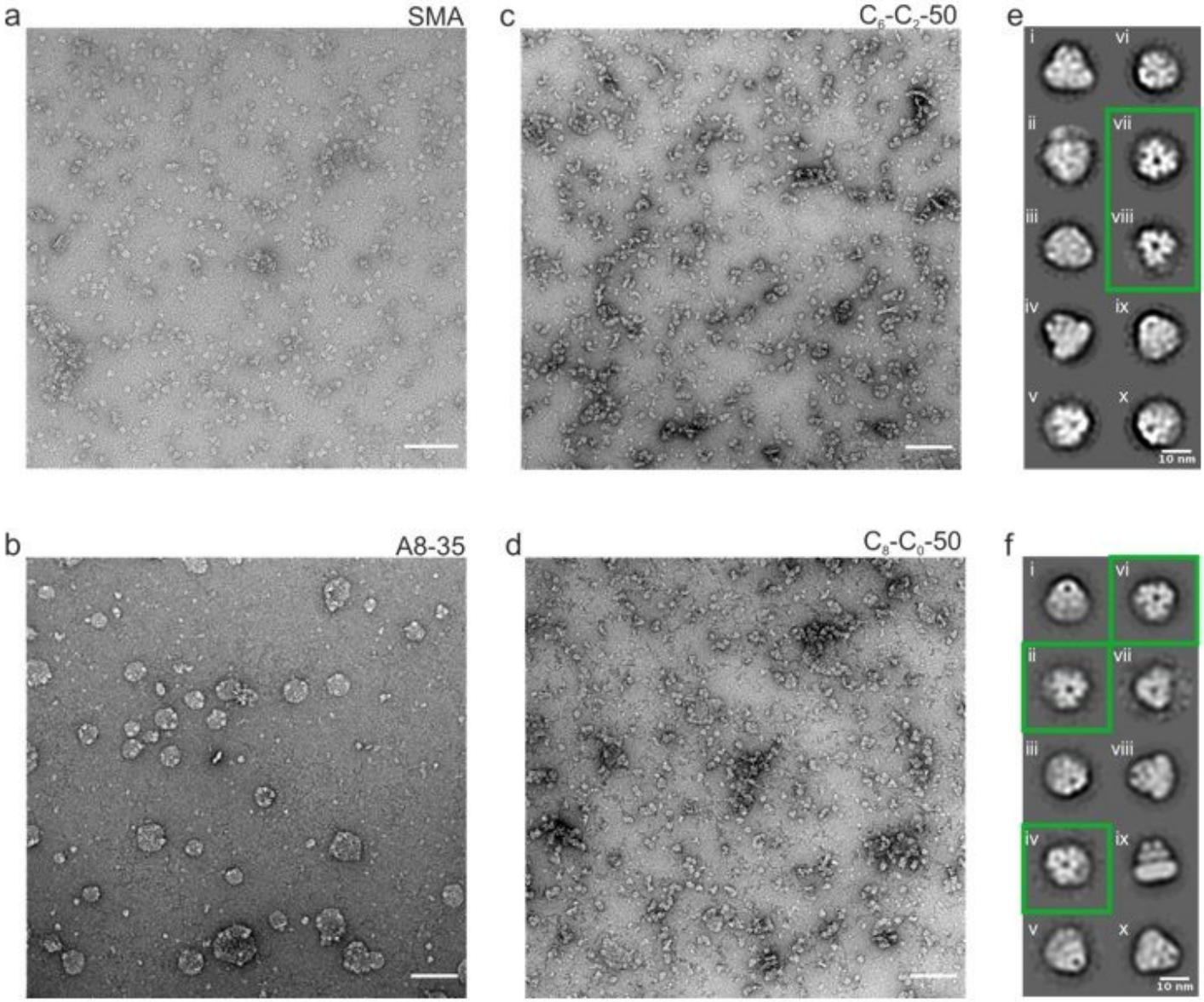

Figure 2

Negative stain electron microscopy of AcrB extracted and purified in SMA, A8-35 and CyclAPols. Representative micrographs were collected at 49k magnification of AcrB following purification in a) SMA b) A8-35 c) C6-C2-50, and d) C8-C0-50. Scale bar is 100 nm in all images. Negative stain 2D classes of AcrB in (e) C6-C2-50 and (f) C8-C0-50 are also shown with representative high-angle classes highlighted in green. Images a and b-d were taken using Tecnai F20 and G2-spirit T12 transmission electron microscopes, respectively.

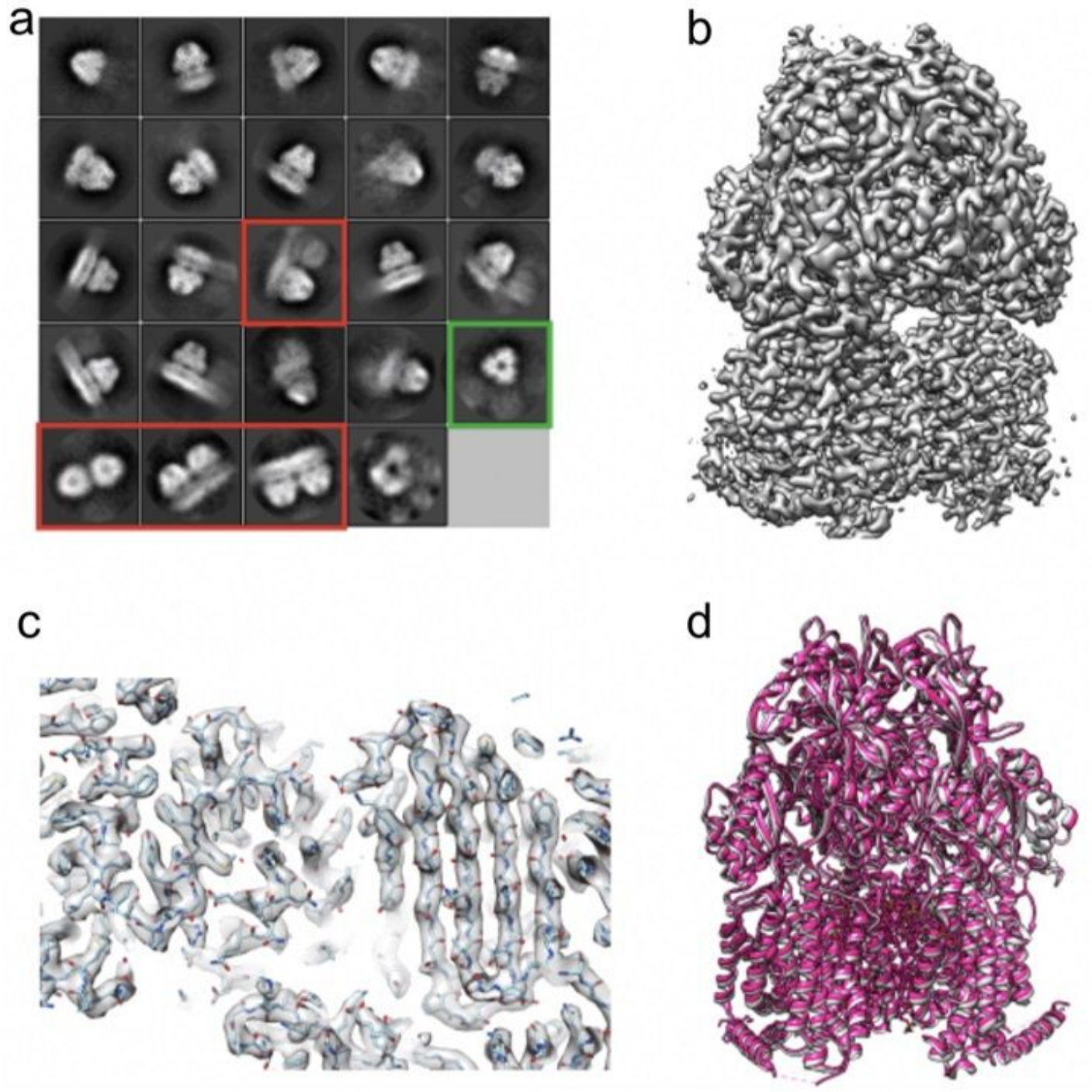

Figure 3

CryoEM of AcrB extracted and purified in CyclAPol C8-C0-50. a) Classes of AcrB in C8-C0-50 following one round of 2D classification. The classes demonstrate a range of views such as high angle view showing putative 3-fold symmetry (highlighted in green) with classes showing doublets highlighted in red. b) Side view of the AcrB cryoEM map at 3.2 Å final resolution. c) Representative map density of AcrB in C8-C0-50 around the vestibule region. d) Overlay of the cryo-EM structure of AcrB in SMA41 (PDB

access code: 6baj; pink) with the new structure (PDB access code 7B5P; grey) demonstrating the close similarity of structures.

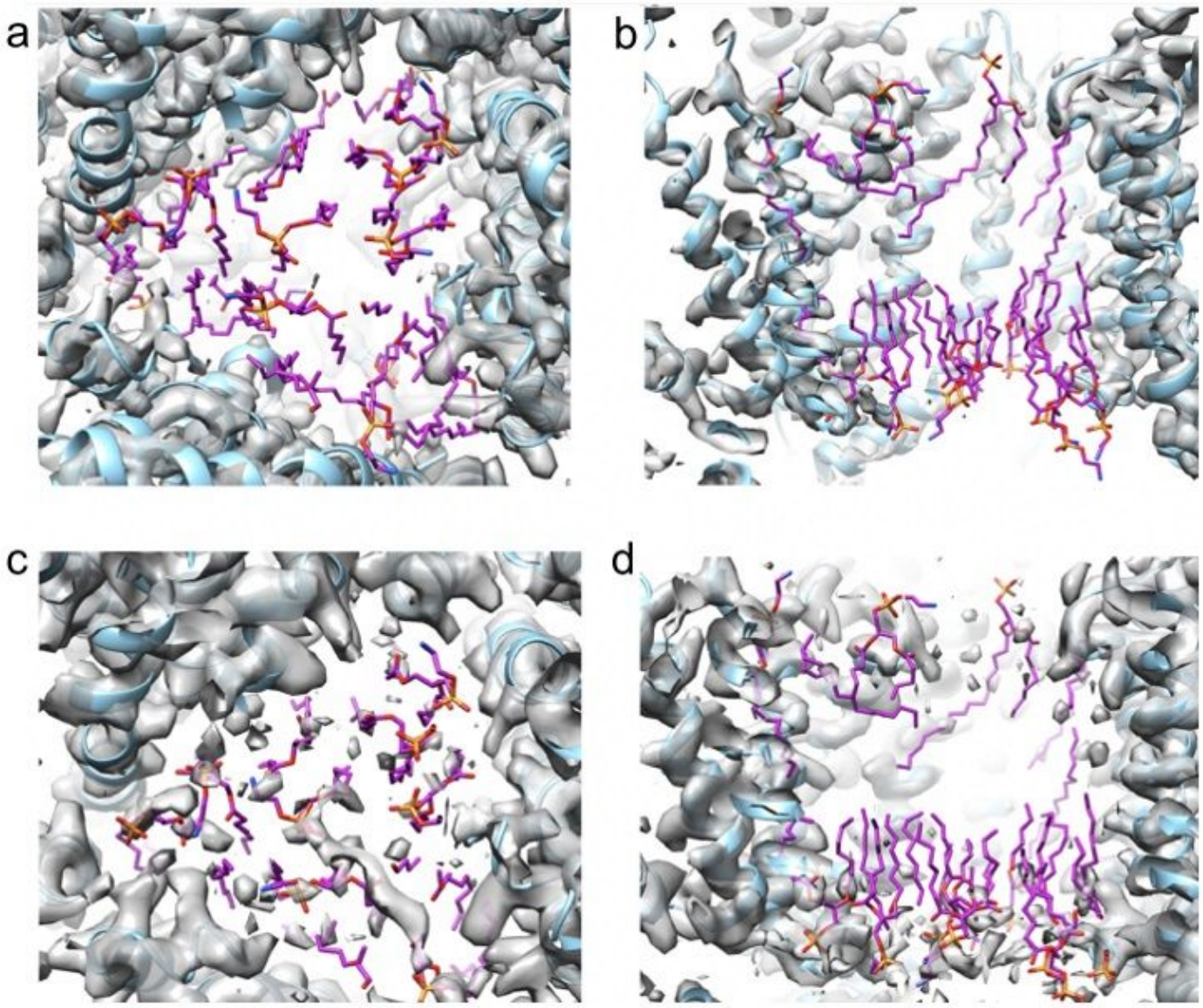

Figure 4

Analysis of the lipid binding site in AcrB. Density map of C8-C0-50-purified AcrB seen around the transmembrane region from the side and base. The lipids from AcrB solved by cryoEM in SMA are superimposed and shown in purple. The density in (a) and (b) is comparable to that of Figure3c (0.235), a lower threshold of density (0.135) shown in (c) and (d) with increased noise also shows no apparent density for the bound lipids.

Supplementary Files

This is a list of supplementary files associated with this preprint. Click to download.

- SupplementaryMaterial.pdf